Relaxation Phenomena in Aqueous Dispersions of Synthetic Lecithins†

Tian Yow Tsong* and Minoru I. Kanehisa

ABSTRACT: The temperature-jump method has been used to study molecular relaxations in aqueous dispersions of synthetic lecithins. They include the relaxations due to the crystalline–liquid crystalline phase transitions of lipid bilayers, changes in the aggregation state of the liposomal structures, and perhaps solvent permeation through the membranes. Kinetics of the upper phase transition of dimyristoyl- and dipalmitoyllecithin dispersions (multilayered liposomes) is complex. Two concentration-independent relaxations, one in the 1-s and the other one in the 0.01-s time ranges, are resolved and examined in detail. Both relaxation times exhibit maxima near the midpoint of the phase transition. An additional reaction in the 10-s time range constitutes about 20% of the total optical change. Experiments with monobilayer vesicles show equally complex kinetics, but the relaxations for the small vesicles are an order of magnitude faster. A cluster model of lipid phase transition in which kinetics of the transition is treated as the rate of the "phase separation" in a two-dimensional lattice qualitatively reproduces the experimental results. When a large temperature perturbation (>5 °C) is applied to the suspension a concentration-dependent relaxation time is detected in the vicinity of the upper phase transition. The reaction probably arises through a reassembly of ruptured bilayer aggregates following a drastic perturbation of the dispersion. This reaction is not observed in suspensions of monobilayer vesicles.

Phospholipids when dispersed in aqueous solutions form various types of bilayer aggregates (Bangham et al., 1965; Huang, 1969). Such phospholipid aggregates have been shown to mimic biological membranes in many regards (Chapman, 1968; Papahadjopoulos and Kimelberg, 1973; Bangham et al., 1965; Yu and Branton, 1976; Michaels et al., 1976; Strittmatter and Rogers, 1975). One of the many interesting physical properties of phospholipid dispersions is the thermotropic phase transition of the lipid molecules (Chapman and Collin, 1965; Chapman, 1968; Hinz and Sturtevant, 1972; Reinert and Steim, 1970; Overath and Träuble, 1973; Melchior et al., 1970; Janiak et al., 1976; Suurkuusk et al., 1976). The existence of lipid phase transitions has been demonstrated also in many plasma membranes (Reinert and Steim, 1970; Melchior et al., 1970; Overath and Träuble, 1973) and in the living cells (Melchior et al., 1970). Although the relation of these phase transitions to the biological functions of cell membranes is not yet clear, it appears that cells can grow only above the lipid phase transition of their plasma membranes (Melchior and Steim, 1976). Moreover, many membrane-associated activities, such as transport of metabolites, enzyme activities, mitochondrial respiration, and surface protein distribution, appear to depend on the crystalline state of membrane lipids (Melchior and Steim, 1976; Linden et al., 1973; Op Den Kamp et al., 1974; Wilson and Fox, 1971; Mavis and Vagelow, 1972).

Many physicochemical methods have been employed to investigate the thermotropic phase transition (Barratt et al., 1969; Hubbell and McConnell, 1968; Sackmann et al., 1973; Hinz and Sturtevant, 1972; Janiak et al., 1976; Hsu and Chan, 1973). Most of these studies have focused on changes in the fluidity or the microviscosity of lipid bilayers associated with the phase transition. Relatively little data are available concerning the relaxation phenomena of phospholipid suspensions (Hammes and Tallman, 1970; Owen et al., 1970; Träuble, 1971; Clegg and Elson, 1975). In a previous communication we have reported a preliminary study of the kinetics of the crystalline–liquid crystalline phase transition of DML[1] bilayers (Tsong, 1974). The present report extends these kinetic measurements to cover the complete temperature range of the phase transitions for DML and DPL dispersions. Relaxations due to other molecular processes, such as self-assembly and solvent permeation, also are examined. In addition, we present a kinetic model, in which the lattice dynamics of the bilayer is treated statistical mechanically.

Materials and Methods

Phospholipid Dispersions. DML and DPL were obtained from Calbiochem. In some experiments the lipids were further purified on a silicic acid column by the method of Robles and Van den Berg (1969). In other experiments the commercial phospholipids were used without purification. Kinetic measurements with the two samples agreed within experimental error.

Two types of phospholipid dispersions were prepared. The first type corresponds to the multilayered liposomes of Bangham et al. (1965). Phospholipids were dispersed in an excess amount of 0.05 M phosphate buffer containing 0.1 N NaCl and 2×10^{-5} M EDTA (pH 7.0) at temperatures a few degrees above the phase transition temperatures, either by hand shaking or by a short period of sonic irradiation (3 min) with a Biosonik IV. The suspension was then incubated at the same temperature for at least 1 h. Without this incubation period the suspension was unstable and often precipitated in the course of experiment. Electron microscopic examination of stable samples indicated that lipid molecules existed in onion-like arrangements.

The second type of lipid dispersions corresponds to the monobilayer vesicles described by Huang (1969). Phospholipid suspended in a well-degassed buffer was placed in a water-

† From the Department of Physiological Chemistry, The Johns Hopkins University School of Medicine, Baltimore, Maryland 21205. *Received January 18, 1977.* This work was supported by National Institutes of Health Grant No. HL 18048 and National Science Foundation Grant No. BMS 75-08690.

[1] Abbreviations used are: DML, dimyristoyl-L-α-lecithin; DPL, dipalmitoyl-L-α-lecithin; Ans, 8-anilino-1-naphthalenesulfonate.

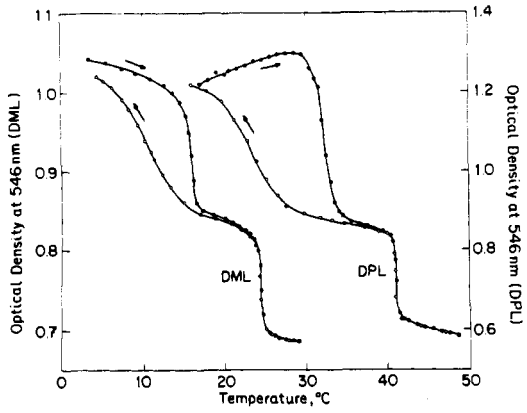

FIGURE 1: Equilibrium melting curves of Bangham type lecithin dispersions. The heating curves are given in the filled circles and the cooling curves are shown in the open circles. Pronounced hysterises are seen for the lower transitions of both DML and DPL dispersions. Conditions: 1 mg/mL each of lipids was dispersed in 0.05 M phosphate buffer at pH 7.0, containing 0.1 N NaCl-20 μM EDTA. A heating and cooling rate of 0.15 °C/min was used. Turbidity changes at 546 nm were monitored. Some numerical values charateristic of these transition curves are given in Table I.

jacketed glass tube and sonicated with a standard titanium probe at 100-W power level for 2 h under nitrogen stream. A time switch set the sonicator alternatively at 15 s on duty and 15 s off duty so that the actual sonication was 1 h. This alternate sonication prevented sample solutions from overheating. After the sonication the solid contamination was removed by spinning the suspension at 20 000g in a Sorvall RC2-B refrigerated centrifuge for 15 min. The suspension was then subject to a chromatographic separation with a 2.5 cm × 30 cm Sepharose 4B column as described by Huang (1969). Two peaks were obtained. The major peak which accounted for more than 90% of the lipid corresponds to the monobilayer vesicles. Electron microscopic examination indicated uniform size vesicles with an average diameter of 250 Å. These small vesicles aggregated slowly at room temperature in the presence of NaCl. Only freshly prepared sample was used in the experiment.

Equilibrium and Kinetic Measurements. Equilibrium transition curves were taken with a McPherson 707K spectrophotometer equipped with a Haake PG 11 temperature programmer. Turbidity changes of lipid suspension were used to monitor the phase transition. A uniform heating rate of 0.2 deg/min was used.

Rapid temperature-jump kinetic measurements were done in a Messanlagen temperature-jump apparatus (Eigen and de Maeyer, 1963). The initial temperature of the solution was measured with a calibrated YSI probe by placing it into a hole in the upper electrode of the temperature-jump cell. The magnitude of the temperature jump was calculated as described previously (Tsong et al., 1976). In order to estimate the amplitude of a very slow reaction (τ_s) an equilibrium transition curve was actually taken with the temperature-jump apparatus. Experimental details of the rapid temperature jump are given elsewhere (Tsong et al., 1976).

Electric dichroic effects were judged to be nonsignificant in this work as none of the relaxations reported here were eliminated by the use of a polarized light source as described by Dourlent et al. (1974). The slow temperature jump was performed with the stopped-flow apparatus by a separate control of the observation chamber and the reservoir temperatures, as described previously (Tsong and Baldwin, 1972).

Results

Equilibrium Transition Curves. Light scattering (90°) or absorbance changes of lipid suspension were used to monitor the crystalline-liquid crystalline phase transition (Yi and MacDonald, 1973; Tsong, 1974). The choice of light scattering change over use of spectroscopic probes such as Ans or bromothymol blue is to avoid confusion of probe binding reactions from the conformational transition of lipid molecules in our relaxation measurements. The turbidity of a lipid suspension reflects an intrinsic property of the bilayer structures (Yi and MacDonald, 1973). However, any morphological change of liposome that may accompany the phase transition of bilayers would contribute to the turbidity of the suspension.

Figure 1 gives the equilibrium melting curves of DML and DPL liposomes. The curves obtained by the elevation of temperature are shown in the filled circles and the curves obtained by the cooling of suspensions are shown in the open circles. The most interesting feature of the figure is the pronounced hysteresis of the lower transitions ($L_{\beta'} \rightarrow P_{\beta'}$).[2] The lower transitions measured by the turbidity have much larger amplitudes compared to those obtained with other methods (Hinz and Sturtevant, 1972; Shimshick and McConnell, 1973). According to Janiak et al. (1976) the lower transition is associated with a structural transformation from a one- to two-dimensional monoclinic lattice consisting of lipid lamellae distorted with a periodic undulation. Thus, the large turbidity change may attribute to a large change in the optical anisotropy of the bilayers (Yi and MacDonald, 1973). However, as can be seen from the heating and the cooling behavior of the transition curves, only by incubating lipid suspensions at temperatures far below the lower transition (T_{m1}) can one regain the full amplitude of the transitions.

This communication will focus on the upper transitions ($P_{\beta'} \rightarrow L_{\alpha}$)[2] shown in Figure 1. The upper transitions correspond to the crystalline-liquid crystalline phase transition of the lipid bilayers (Chapman and Collin, 1965; Hinz and Sturtevant, 1972; Janiak et al., 1976). No hysteresis had been found if the heating and cooling rate was kept low at 0.2 °C/min and the temperature of the solution was monitored directly. The transition curves obtained by the turbidity measurements are among the sharpest reported for DPL and DML suspensions. Some numerical values which characterize these transition curves are given in Table I.

In the table, the midpoint of transition, T_m, was taken as the temperature where the transition curve exhibited the maximum slope, $d\theta/dT$. $(d\theta/dT)_{T=T_m}$ and the van't Hoff enthalpy, ΔH_{vH}, were obtained by the graphical analysis of the transition curves as outlined elsewhere (Tsong et al., 1970). Both $(d\theta/dT)_{T=T_m}$ and ΔH_{vH} are good measures of the cooperativity of the phase transition (Mabrey and Sturtevant, 1976; Hinz and Sturtevant, 1972; Tsong, 1974). However, the use of the ratio $\Delta H_{vH}/\Delta H_{cal}$ (where ΔH_{cal} is the calorimetrically measured ΔH) for the estimation of the cooperative unit, as has been done by many authors, needs further assessment (Kanehisa and Tsong, 1977) and is not given here. The data for the multilayered liposomes of DPL and DML are in a good agreement with the calorimetric results (Mabrey and Sturtevant, 1976) except that in our case T_{m1} is 1 °C higher for DML

[2] The designation of the lower and the upper transitions follows Janiak et al. (1976) and Tardieu et al. (1973). The nomenclature is that of Luzzati (1968): L and P denote, respectively, a one-dimensional lamellar lattice and a two-dimensional monoclinic lattice; α and β' represent, respectively, a hydrocarbon chain conformation in a liquid paraffin-like arrangement and crystalline-like chains tilted with respect to the bilayer plane. For a pictorial presentation see Figure 7 of Janiak et al. (1976).

TABLE I: Some Numerical Values for the Equilibrium Crystalline–Liquid Crystalline Phase Transition of Aqueous Dispersion of Lecithins.[a]

	Lower transition ($L_{\beta'} \rightarrow P_{\beta'}$)			Upper transition ($P_{\beta'} \rightarrow L_{\alpha}$)		
	T_{m1} (°C)	$(d\theta/dT)$ $(T = T_{m1})$ (deg^{-1})	ΔH_{vH} (T_{m1}) $(10^6$ cal/mol)	T_{m2} (°C)	$(d\theta/dT)$ $(T = T_{m2})$ (deg^{-1})	ΔH_{vH} (T_{m2}) $(10^6$ cal/mol)
Bangham type liposome						
DML (heating)	15.8	0.67	0.44	24.4	2.5	1.76
DML (cooling)	10.0	0.13	0.083	24.3	2.4	1.69
DPL (heating)	32.2	0.42	0.31	41.2	2.8	2.20
DPL (cooling)	23.5	0.13	0.091	41.0	2.8	2.20
Monobilayer vesicles						
DML (heating and cooling)		Not observed		19.0	0.20	0.14
DPL (heating and cooling)		Not observed		36.5	0.40	0.30

[a] Conditions were: 0.1 N NaCl–20 μM EDTA–0.05 M phosphate buffer at pH 7.0. $\Delta H_{vH} = 4RT_m^2(d\theta/dT)_{T=T_m}$, where θ denotes the order parameter.

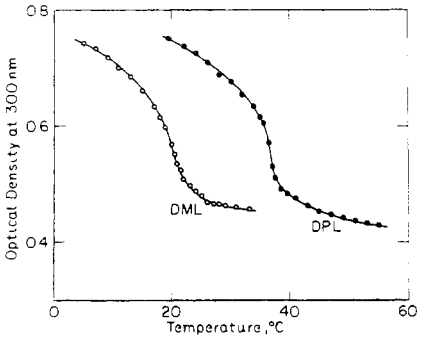

FIGURE 2: Equilibrium transition curves of monobilayer lecithin vesicles. Only the heating curves are shown. The lipid concentration was 10 mg/mL in each case. Turbidity changes at 300 nm were monitored. Other experimental conditions are the same as in Figure 1. Numerical values characteristic of the transition curves are given in Table I.

and is 3 °C lower for DPL. The source of this discrepancy is unknown.

In contrast to the transition curves of Bangham type liposomes transition curves obtained for the monobilayer vesicles are monotonic in feature, as shown in Figure 2. There is only one transition which is reversible. The midpoint of this phase change occurs at 19 °C for DML and at 37 °C for DPL vesicles. The turbidity at 500 nm of the monobilayer vesicles is less than 5% that of Bangham type liposomes at the same lipid concentration. The small vesciles slowly aggregate in the presence of NaCl, but do not fuse appreciably since the turbidity change due to the aggregation reaction was only about 1.5- to 3-fold. A complete fusion of small vesicles to Bangham type liposome would have increased the turbidity by at least 2000%. The use of NaCl in the suspension is essential for the temperature-jump experiment. Some numerical values of the transition curves shown in Figure 2 are given in Table I to be compared with the curves given in Figure 1.

The values of $(d\theta/dT)_{T=T_m}$ and ΔH_{vH} for the monobilayer vesicles are subject to a larger uncertainty owing to the difficulty in determining pretransition baseline. The transition is tentatively assigned to $P_{\beta'} \rightarrow L_{\alpha}$ for the following reasons: (1) the transition is readily reversible and exhibits no hysteresis; (2) for lipid samples with an increased degree of sonication the T_{m2} gradually approaches that of the monobilayer vesicles. Likewise, there is a gradual diminishing of the lower transition by the extensive sonication.

Kinetics of the Crystalline–Liquid Crystalline Phase Transition. The Joule-heating temperature-jump method of Eigen and de Maeyer (1963) requires passage of electric current through the solution. It has been observed that a high-voltage pulsation of an erythrocyte suspension leads to a change in the permeability of the red cell membranes (Tsong et al., 1976; Kinosita and Tsong, 1977). Because of the possible complication of electric field extreme precaution has to be taken to separate reactions of different molecular natures. When relaxations due to the phase transition are to be studied the field effect can be kept at minimum by using a small temperature perturbation ($\Delta T < 1$ °C; see Tsong et al. (1976) for details). The only reaction, beside the phase transition, that cannot be eliminated is a very fast reaction (τ_f) in the microsecond time range, which is observed at any condition studied. The amplitude of the τ_f reaction depends on the perturbation size and is insignificant (<5%) when the small temperature jump is employed in studying the phase transition of the liposomes.

Figures 3a and b give oscilloscope records of DML upper phase transition (Bangham type liposomes) measured by the turbidity changes of the suspension at 500 nm. It is clear that the kinetics is complex, and can be resolved into at least two relaxation times, one in the 0.01-s time range (τ_2) and the other in the 1-s time range (τ_1). About 20% of the equilibrium optical change is not accounted for and is attributed to an even slower reaction in the 10-s time range (τ_s). The presence of τ_s reaction has been confirmed in a slow temperature-jump experiment with a stopped-flow apparatus. Only τ_1 and τ_2 reactions have been examined in detail (Table II).

Both τ_1 and τ_2 reactions are independent of the lipid concentration in the range of 0.2 to 2 mM (Figure 4, right panel). The left panel indicates that the total signals of the two reactions, on the other hand, depend linearly upon the lipid concentration, ensuring again that complication due to aggregation reaction is not serious if present at all. The most interesting feature of these two reactions is the occurrence of maxima near the phase transition temperature (T_{m2}), as shown in Figure 5. This result contrasts sharply with the data of the molecular permeation experiments reported by Tsong (1975a,b) and Marsh et al. (1976). In these experiments the permeation of certain dyes and spin-labels was shown to exhibit minimum time constants at the T_{m2}.

The relaxation measurement was extended to include Bangham type liposomal suspension of DPL, and the result is

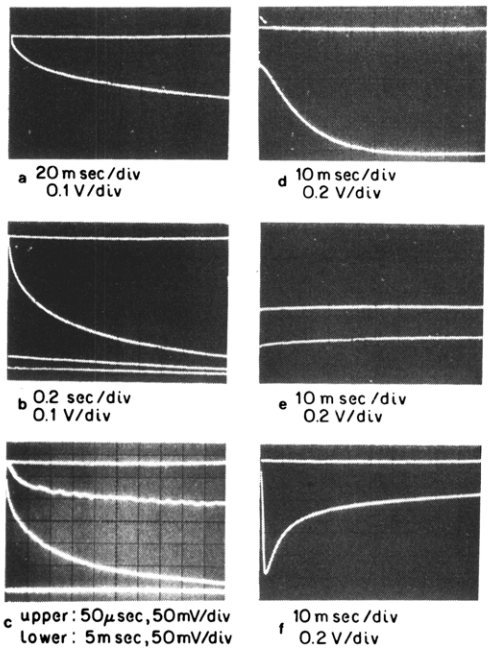

FIGURE 3: Temperature-jump relaxations of lecithin suspensions. (a) The rapid kinetic phase (τ_2) of the crystalline–liquid crystalline phase transition of DML (Bangham type liposomes): temperature jump, 24.0 to 24.2 °C, lipid concentration, 2 mg/mL, turbidity at 500 nm was used. (b) The slow kinetic phase (τ_1) of the phase transition. The experimental conditions are the same as in a. (c) The kinetics of the crystalline–liquid crystalline phase transition of DPL monobilayer vesicles: lipid concentration, 15 mg/mL; temperature jump, 36.0 to 37.0 °C; turbidity at 300 nm was used to monitor the reaction. (d) The first temperature-jump measurement of the lower transition of Bangham type DML dispersion: temperature jump 14 to 16 °C. The sudden drop in the signal is due to a very rapid reaction (τ_f) discussed in the text. Other experimental conditions are the same as in a. (e) The second temperature jump of the lower transition. Because of the hysteresis the phenomena signal observed in d is missing here. Long incubation of the sample at 5 °C gave back the signal. (f) Signals generated by a large temperature jump (35 to 40 °C) of DPL dispersions (Bangham type). The rapid drop in turbidity is the result of membrane ruptures plus τ_f reaction. The slower return of the turbidity is interpreted as due to a reassembly of the bilayers. The reassembly reaction is lipid concentration dependent as shown in Figure 6. Other experimental conditions are the same as in a. All experiments were done in 0.05 M phosphate buffer at pH 7.0, containing 0.1 N NaCl and 20 μM EDTA.

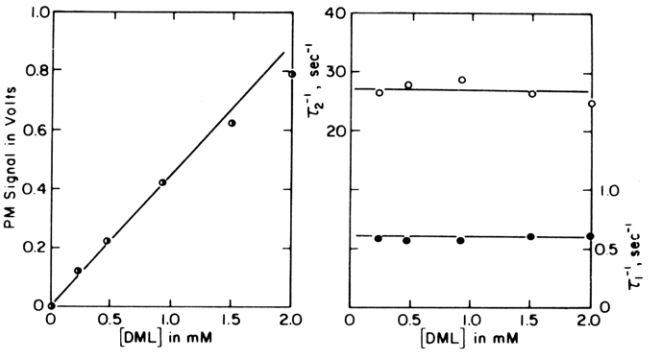

FIGURE 4: Concentration dependence of the relaxation times for the crystalline–liquid crystalline phase transition of DML. In order to ensure that the τ_1 and τ_2 reactions presented here do not result from changes in the aggregation state of the liposomes the relaxation measurement was done in the concentration range of 2.0 to 0.2 mM. The left panel indicates that the total signal is linearly proportional to the DML concentration, but not the relaxation times (right panel): temperature jump 24.0 to 24.2 °C.

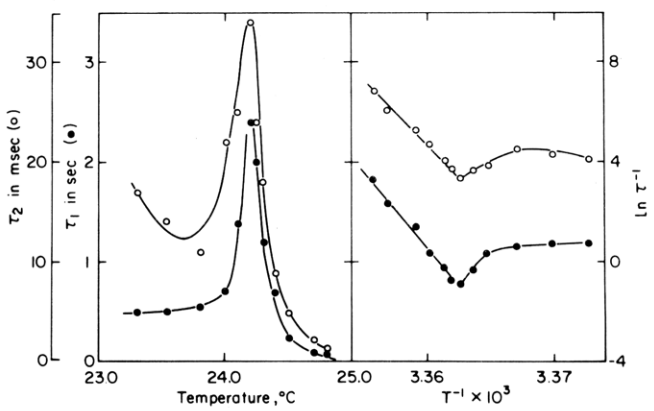

FIGURE 5: Temperature dependence of the relaxation times for the crystalline–liquid crystalline phase transition of DML. The left panel shows that both the rapid (τ_2) and the slow (τ_1) reactions exhibit maxima at the transition temperature (24.2 °C). The right panel gives curves equivalent to Arrhenius plots. See text for details.

given in Table II. As is expected the data resemble, in most aspects, that of DML dispersions except that τ_2 is slower and τ_1 is slightly faster for DPL. Both relaxations exhibit maxima around 41 °C (see Table II) which is the upper phase transition temperature of DPL.

We have not done a systematic study on the monobilayer vesicles of DML and DPL owing to the following reasons. (i) These vesicles are not stable and aggregate slowly in the upper phase transition region. (ii) The transition curves are broad (Figure 2). Thus, it requires a larger temperature perturbation to obtain good signals. This also introduces signals that result from the electric field induced permeation of solvent (Tsong et al., 1976; Kinosita and Tsong, 1977). (iii) The complexity of the kinetics observed in the Bangham type liposomes is also seen here although τ_1 and τ_2 reactions are an order of magnitude faster in the case of small vesicles. Thus kinetics of the phase transition in the small vesicle system is qualitatively similar to that of multilayered liposomes. As an example an oscillograph record of the kinetics of the phase transition of DPL small vesicles is given in Figure 3c.

It has been suggested (Tsong, 1974) that the complex kinetics of the lipid phase transition may reflect a heterogeneous size distribution of liposomal preparation. The above experiment makes this interpretation unlikely. Even if there is a small fraction of lipid molecules in the form of small vesicles their contribution to the turbidity change of the liposome suspension would be negligible. As will be shown in the Discussion section the complex kinetic behavior may be expected with a model of the lattice dynamics of the bilayer structures.

Other Relaxation Processes. Kinetics of the lower phase transition of DML liposomes occurs in the 10-ms time range. The reaction is irreversible because of the hysteresis of the transition (Figure 1). Oscillograph d of Figure 3 illustrates the first temperature jump of a DML dispersion from 14 to 16 °C. A sudden drop in the signal is due to τ_f reaction mentioned previously. The signal that followed gives the kinetics of $L_{\beta'} \rightarrow P_{\beta'}$ transition. After the measurement the sample was kept in the temperature-jump cell until the temperature returned to 14 °C and a second jump of temperature was done. No signal was detected as shown in Figure 3e. This is expected if the signal indeed comes from the lower transition. Incubation of the sample at 5 °C for 10 min gave back the signal.

The τ_f reaction was detected in all temperature ranges. Thus, it does not belong to the upper phase or the lower phase transitions. The reaction occurs in the 50 μs time range and is independent of the lipid concentration. It has an activation energy of 11 kcal/mol for DML (τ_f = 55 μs at 25 °C) and 12 kcal/mol for DPL (τ_f = 85 μs at 25 °C) suspensions. A similar

TABLE II: Rapid Kinetics of the Uppper Phase Transition ($P_{\beta'} \rightarrow L_\alpha$) of Bangham Type Lecithin Dispersions.[a]

DML						DPL					
T_i (°C)	T_f (°C)	τ_1 (s)	τ_2 (ms)	α_1 (%)	α_2 (%)	T_i (°C)	T_f (°C)	τ_1 (s)	τ_2 (ms)	α_1 (%)	α_2 (%)
23.0	23.3	0.50	17	60	40	39.6	40.1	0.25	32	75	25
23.3	23.6	0.50	14	53	47	39.8	40.3	0.20	44	75	25
23.5	23.8	0.55	11	46	54	40.1	40.6	0.34	56	73	27
23.7	24.0	0.70	22	41	59	40.3	40.8	0.41	62	74	26
23.9	24.1	1.4	25	32	68	40.5	41.0	0.44	70	65	35
24.0	24.2	2.4	34	29	71	40.7	41.2	0.32	68	67	33
24.05	24.25	2.1	24	29	71	40.9	41.4	0.34	45	63	37
24.1	24.3	1.2	18	47	53	41.0	41.5	0.30	26	63	37
24.2	24.4	0.70	9.0	52	48	41.1	41.6	0.35	22	67	33
24.3	24.5	0.25	5.0	50	50	41.2	41.7	0.30	18	67	33
24.5	24.7	0.10	2.3	50	50	41.3	41.8	0.25	10	71	29
24.5	24.8	0.08	1.4	55	45	41.4	41.9	0.24	9	77	23

[a] Conditions were: 0.1 N NaCl-20 μM EDTA-0.05 M phosphate buffer at pH 7.0. Lipid concentration was 2 mg/mL in each case. Turbidity at 500 nm was used to follow the reactions. In the estimation of α_1 and α_2, the fractions of reaction which occur in τ_1 and τ_2 kinetic phases, respectively, signals due to τ_f and τ_s reactions (see text) are not considered. T_i and T_f denote, respectively, temperatures before and after the temperature jump.

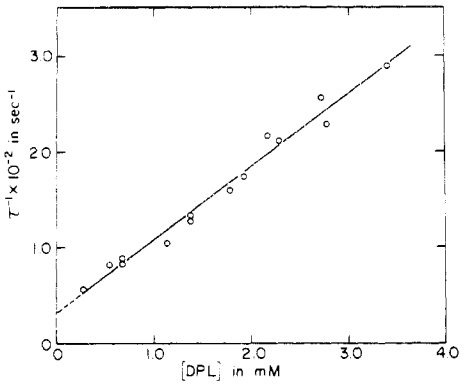

FIGURE 6: Concentration dependence of the reassembly reaction shown in Figure 3f for DPL at 40 °C. A simple aggregation mechanism:

$$A + A \underset{k_b}{\overset{k_f}{\rightleftharpoons}} A_2$$

yields $k_f = 7.5 \times 10^4\ M^{-1}\ s^{-1}$ and $k_b = 20\ s^{-1}$.

reaction has also been detected in erythrocyte and in ghost suspensions (Tsong et al., 1976). The reaction has been interpreted as due to the movement of solvent molecules in the membraneous structures (Owen et al., 1970; Tsong et al., 1976).

When a large temperature jump (>5 °C) is applied to the Bangham type liposome suspensions of DPL and DML in the vicinity of the upper phase transitions, signals resembling oscillograph f of Figure 3 were obtained. A rapid decrease in turbidity (too fast to be resolved) is followed by a slower return of the turbidity to nearly its initial value. The return of the turbidity occurs in the millisecond time range and its relaxation time depends linearly on the lipid concentration (Figure 6). The reaction is found only in the range of the upper transitions and is absent in monobilayer vesicle suspensions. These observations suggest that the signal detects a reassembly reaction of either thermally or electrically ruptured bilayer membranes (Tsong et al., 1976; Kinosita and Tsong, 1977). Since the signal of this reaction overlaps with the bilayer phase transition a precise measurement of the relaxation cannot be done in the transition zone. Nevertheless, it has been observed that at temperatures far removed from T_{m2} the assembly reaction becomes extremely slow. The rupture reaction was always detected in liposome suspensions in the large temperature-jump experiments. Signals due to membrane rupture and reassembly of bilayers have not been detected in the small temperature jump (<2 °C) experiment.

Discussion

Kinetic Model of Lipid Phase Transition. The kinetic scheme we are proposing here for the interpretation of the relaxation data is based on a cluster model of lipid-phase transition recently being developed in our laboratory (Fisher, 1967; Kanehisa and Tsong, 1977; Tsong et al., 1977). The model treats the lipid bilayer as an idealized two-dimensional Ising lattice. A lipid molecule is allowed to exist only in two states, namely, the solid-like state (S state) and the fluid-like state (F state). When the system approaches the transition temperature, T_m, from S state certain molecular clusters, composed of lipid molecules in F state linked together by the nearest neighbors, begin to appear and grow in the predominant phase of S state. No information on the detailed configurational change of lipid molecules is required for the formulation. In other words, the model focuses only on the lattice dynamics of the bilayers.

Kinetics of the phase transition is equivalent to the rate of the formation of lipid clusters. In the simplified version in which coalescence and splitting off among clusters are ignored kinetics of the cluster reaction can be described by eq 1:

$$C_0 \underset{b_1}{\overset{\sigma}{\rightleftharpoons}} C_1 \underset{b_2}{\overset{f_1}{\rightleftharpoons}} C_2 \underset{b_3}{\overset{f_2}{\rightleftharpoons}} \cdots \underset{b_l}{\overset{f_{l-1}}{\rightleftharpoons}} C_l \cdots \qquad (1)$$

nucleation and annihilation — growth and shrinking

In the scheme C_l represents a cluster composed of l lipid molecules, and σ, f_l, and b_l denote, respectively, the rate constants for the nucleation, the growth, and the shrinking of the cluster. f_l and b_l depend on the size l and assume the relationships (Kanehisa and Tsong, 1977):

$$\left.\begin{aligned} f_l &= f_1 l^r \\ b_l &= b_1 l^r \end{aligned}\right\} \text{ where } \tfrac{1}{2} \lesssim r \qquad (2)$$

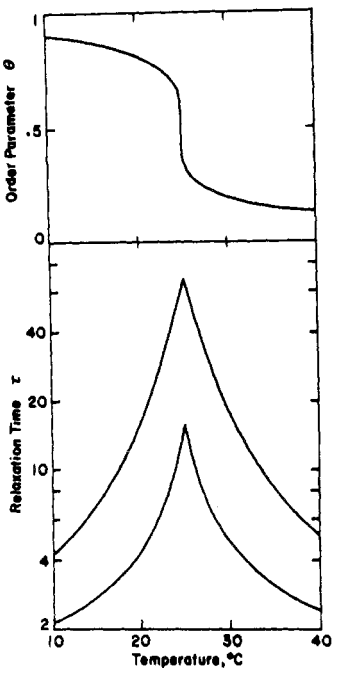

FIGURE 7: Relaxation times for the linear cluster reaction given in eq 1. The upper panel gives an equilibrium transition curve, with T_m at 25.0 °C, for the two-dimensional Ising lattice according to a cluster model of lipid phase transition (Kanehisa and Tsong, 1977). The lower panel gives the relaxation times of eq 1. The cluster reaction was truncated at l_{max} = 50 and the rate constant b_1 was assumed to be unity. Other rate constants were determined so as to satisfy the equilibrium conditions of eq 4 and 5, and with $r = 8/15$ (see eq 2). The two relaxation times shown are the mean relaxation time of Schwartz (1965) (upper curve) and the reciprocal of the smallest eigenvalue (lower curve), which are thought to correspond to the initial and the final slopes of the experimental relaxation curve. The relaxation amplitudes for the slowest rate from the completely ordered state to temperatures 15, 20, 23, 24, 24.5, and 29 °C were, respectively, 23, 27, 49, 63, 71, and 77%. The relaxation amplitude for each mode of reaction depends on the l_{max} value chosen. The amplitude of the slowest reaction becomes smaller when l_{max} becomes larger.

If the concentration of l size cluster in mole fraction is denoted by n_l, after the temperature jump n_l as a function of time may be obtained by solving the set of differential equations:

$$\begin{aligned} \frac{dn_0}{dt} &= -\sigma n_0 + b_1 n_1 \\ \frac{dn_1}{dt} &= \sigma n_0 - (b_1 + f_1) n_1 + b_2 n_2 \\ \frac{dn_l}{dt} &= f_{l-1} n_{l-1} - (b_l + f_l) n_l + b_{l+1} n_{l+1} \end{aligned} \tag{3}$$

At equilibrium the following relations hold for the system:

$$\frac{\sigma \bar{n}_0}{b_1 \bar{n}_1} = \frac{f_1 \bar{n}_1}{b_2 \bar{n}_2} = \ldots = \frac{f_{l-1} \bar{n}_{l-1}}{b_l n_l} \tag{4}$$

so that

$$\sigma = b_1 \frac{\bar{n}_1}{\bar{n}_0} \qquad f_l = b_{l+1} \frac{\bar{n}_{l+1}}{\bar{n}_l} \tag{5}$$

The solution to eq 3 can be expressed as:

$$n_l(t) = \bar{n}_l + \sum_{j=1}^{l_{max}} \beta_j^{(l)} e^{-t/\tau_j} \tag{6}$$

where the bar signs specify the equilibrium concentrations. The τ_j are the relaxation times of the system and depend only on the final temperature. The amplitudes $\beta_j^{(l)}$, on the other hand, depend on both the initial and the final temperatures. Equation 3 can also be expressed in matrix form:

$$\dot{\mathbf{n}} = \mathbf{M}\mathbf{n} \tag{7}$$

and the relaxation times and the amplitudes are easily obtained by the diagonalization of the matrix **M**.

The order parameter, θ, of the system at time t is simply:

$$\theta(t) = \begin{cases} 1 - \sum_{l=1}^{l_{max}} l n_l(t) & \text{below } T_m \\ \sum_{l=1}^{l_{max}} l n_l(t) & \text{above } T_m \end{cases} \tag{8}$$

Equation 8 describes the time course of the lipid phase transition after the temperature jump. Note that the above formulation is valid only for a temperature jump within either half of the transition region.

The interesting feature of the cluster model is that it treats the phase transition as a process of phase separation. The method developed here is thus equally applicable to the phase separation phenomena in multicomponent systems (Shimshick and McConnell, 1973; Mabrey and Sturtevant, 1976).

Figure 7 gives the results of a sample calculation of the relaxation times of the cluster formation. In the calculation l_{max}, the maximum size of the cluster is limited to 50. In reality l_{max} can be much larger. The result indicates that the model exhibits a complex kinetics which is dominated by the slowest phase. Several faster modes, closely spaced, show measurable amplitudes. These modes are combined to give a rapid kinetic phase. The sample calculation indicates that both the slow and the fast kinetic phases exhibit maximum relaxations at the T_m, consistent with the experimental observations for the kinetics of the lecithin phase transitions.

References

Bangham, A. D., Standish, M. M., and Watkins, J. C. (1965), *J. Mol. Biol. 13,* 238.

Barratt, M. D., Green, D. K., and Chapman, D. (1969), *Chem. Phys. Lipids 3,* 140.

Chapman, D. (1968), *Biol. Membr. 1,* 125.

Chapman, D., and Collin, D. T. (1965), *Nature (London) 206,* 189.

Clegg, R. M., and Elson, E. L. (1975), *Biopolymers 14,* 883.

Dourlent, M., Hogrel, J. F., and Hélène, C. (1974), *J. Am. Chem. Soc. 96,* 3398.

Eigen, M., and de Maeyer, L. C. (1963), *Tech. Org. Chem. 8,* 845.

Fisher, M. E. (1967), *Physics 3,* 255.

Hammes, G. G., and Tallman, D. E. (1970), *J. Am. Chem. Soc. 92,* 6042.

Hinz, H.-J., and Sturtevant, J. M. (1972), *J. Biol. Chem. 247,* 6071.

Hsu, M., and Chan, S. I. (1973), *Biochemistry 12,* 3872.

Huang, C. (1969), *Biochemistry 8,* 344.

Hubbell, W. L., and McConnell, H. M. (1968), *Proc. Natl. Acad. Sci. U.S.A. 61,* 12.

Janiak, M. J., Small, D. M., and Shipley, G. G. (1976), *Biochemistry 15,* 4575.

Kanehisa, M. I., and Tsong, T. Y. (1977), manuscript in preparation.

Kinosita, K., and Tsong, T. Y. (1977), *Proc. Natl. Acad. Sci. U.S.A.* (in press).

Linden, C. D., Wright, K. L., McConnell, H. M., and Fox, C.

F. (1973), *Proc. Natl. Acad. Sci. U.S.A. 70,* 2271.
Mabrey, S., and Sturtevant, J. M. (1976), *Proc. Natl. Acad. Sci. U.S.A. 73,* 3862.
Marsh, D., Watts, A., and Knowles, P. F. (1976), *Biochemistry 15,* 3570.
Mavis, R. D., and Vagelow, P. R. (1972), *J. Biol. Chem. 47,* 652.
Melchior, D. L., Morowitz, H. J., Sturtevant, J. M., and Tsong T. Y. (1970), *Biochim. Biophys. Acta 219,* 114.
Melchior, D. L., and Steim, J. M. (1976), *Annu. Rev. Biophys. Bioeng. 5,* 205.
Michaels, D. W., Abramovitz, A. S., Hammer, C. H., and Mayer, M. M. (1976), *Proc. Natl. Acad. Sci. U.S.A. 72,* 2852.
Op Den Kamp, J. A. F., De Gier, J., and Van Deenen, L. L. M. (1974), *Biochim. Biophys. Acta 345,* 253.
Overath, P., and Träuble, H. (1973), *Biochemistry 12,* 2625.
Owen, J. D., Hemmes, P., and Eyring, E. M. (1970), *Biochim. Biophys. Acta 219,* 276.
Papahadjopoulos, D., and Kimelberg, H. K. (1973), *Prog. Surf. Sci. 4,* 141.
Reinert, J. C., and Steim, J. M. (1970), *Science 168,* 1580.
Robles, E. C., and Van den Berg, D. (1969), *Biochim. Biophys. Acta 187,* 520.
Sackmann, E., Träuble, H., Galla, H.-J., and Overath, P. (1973), *Biochemistry 12,* 5360.
Shimshick, E. J., and McConnell, H. M. (1973), *Biochemistry 12,* 2351.
Strittmatter, P., and Rogers, M. J. (1975), *Proc. Natl. Acad. Sci. U.S.A. 72,* 2658.
Suurkuusk, J., Lentz, B. R., Barenholz, Y., Biltonen, R. L., and Thompson, T. E. (1976), *Biochemistry 15,* 1393.
Schwartz, G. (1965), *J. Mol. Biol. 11,* 64.
Tardieu, A., Luzzati, V., and Reman, F. C. (1973), *J. Mol. Biol. 75,* 711.
Träuble, H. (1971), *Naturwissenschaften 58,* 277.
Tsong, T. Y. (1974), *Proc. Natl. Acad. Sci. U.S.A. 71,* 2684.
Tsong, T. Y. (1975a), *Biochemistry 14,* 5409.
Tsong, T. Y. (1975b), *Biochemistry 14,* 5415.
Tsong, T. Y., and Baldwin, R. L. (1972), *J. Mol. Biol. 69,* 145.
Tsong, T. Y., Greenberg, M., and Kanehisa, M. I. (1977), *Biochemistry 16* (in press).
Tsong, T. Y., Hearn, R. P., Wrathall, D. P., and Sturtevant, J. M. (1970), *Biochemistry 9,* 2667.
Tsong, T. Y., and Kingsley, E. (1975), *J. Biol. Chem. 250,* 786.
Tsong, T. Y., Tsong, T. T., Kingsley, E., and Siliciano, R. (1976), *Biophys. J. 16,* 1091.
Wilson, G., and Fox, C. F. (1971), *J. Mol. Biol. 55,* 49.
Yi, P. N., and MacDonald, R. C. (1973), *Chem. Phys. Lipids 11,* 114.
Yu, J., and Branton, D. (1976), *Proc. Natl. Acad. Sci. U.S.A. 73,* 3891.

Substrate Selectivity of Squalene Synthetase†

Paul R. Ortiz de Montellano,* Jeng Shu Wei, Wayne A. Vinson, Rafael Castillo, and Amrit S. Boparai

ABSTRACT: Six 1-^{3}H-labeled analogues of farnesyl pyrophosphate have been studied as potential substrates for yeast and rat liver squalene synthetases: 2-methylfarnesyl pyrophosphate (**4**), 3-demethylfarnesyl pyrophosphate (**5**), 7,11-dimethyl-3-ethyl-2,6,10-dodecatrienyl pyrophosphate (**6**), 6,7,10,11-tetrahydrofarnesyl pyrophosphate (**7**), 4-methylthiofarnesyl pyrophosphate (**8**), and 4-fluorofarnesyl pyrophosphate (**9**). Analogues **4** and **5** are enzymatically incorporated into 11-methylsqualene (**10**) and 10-demethylsqualene (**11**), respectively, even if no farnesyl pyrophosphate is *added* to the incubations. None of the other analogues gives nonpolar products with either the yeast or liver enzymes. No tritium is enzymatically released to the medium from any of the analogues, indicating that they are not accepted at the first (proton exchanging) site. The data rule out formation of dead-end presqualene pyrophosphate products with analogues as first, but not as second, substrates. Implications of these results for the enzyme active-site topology and mechanism are discussed.

The biosynthesis of squalene (**3**) from two molecules of farnesyl pyrophosphate (**1**) is a surprisingly complicated process. During the condensation reaction a proton on the pyrophosphate bearing carbon of one of the two identical substrate units is replaced by a hydrogen from NADPH[1] (Popjak et al., 1961, 1962; Childs and Bloch, 1962). This proton exchange, which is not subject to an isotope effect (Popjak et al., 1962), was elegantly shown to occur with a net retention of configuration, while displacement of the pyrophosphate group from the nonexchanging substrate unit occurs with a net inversion of configuration (Cornforth et al., 1966a,b). The complexity implied by asymmetric proton exchange was substantiated on isolation (Rilling, 1966) and structural characterization (Epstein and Rilling, 1970; Popjak et al., 1973; Altman et al., 1971; Coates and Robinson, 1971) of presqualene pyrophosphate (**2**), a discrete intermediate in the enzymatic process (Muscio et al., 1974). Squalene synthetase, the membrane-bound reaction catalyst, has been isolated in soluble form from yeast (Schechter and Bloch, 1971; Qureshi et al., 1973b), and

† From the Department of Pharmaceutical Chemistry, School of Pharmacy, University of California, San Francisco, California 94143. *Received January 10, 1977.* This research was supported by Grant No. HL 15476 from the National Institutes of Health.

[1] Abbreviations used are: $NADP^+$, NADPH, oxidized and reduced nicotinamide adenine dinucleotide phosphate; TLC, thin-layer chromatography; GLC, gas-liquid chromatography.